CHINESE OPTICS LETTERS

Vol. 19, No. 12 | December 2021

Population dynamics of ultra-cold atoms interacting with radiation fields in the presence of inter-atomic collisions

E. Ghasemian and M. K. Tavassoly*

Optic and Laser Group, Faculty of Physics, Yazd University, Yazd, Iran

*Corresponding author: mktavassoly@yazd.ac.ir

Received April 16, 2021 | Accepted June 18, 2021 | Posted Online September 6, 2021

We investigate the dynamics of a system that consists of ultra-cold three-level atoms interacting with radiation fields. We derive the analytical expressions for the population dynamics of the system, particularly, in the presence and absence of nonlinear collisions by considering the rotating wave approximation (RWA). We also reanalyze the dynamics of the system beyond RWA and obtain the state vector of the system to study and compare the time behavior of population inversion. Our results show that the system undergoes two pure quantum phenomena, i.e., the collapse–revival and macroscopic quantum self-trapping due to nonlinear collisional interactions. The occurrence of such phenomena strongly depends on the number of atoms in the system and also the ratio of interaction strengths in the considered system. Finally, we show that the result of the perturbed time evolution operator up to the second-order is in agreement with the numerical solution of the Schrödinger equation. The results presented in the paper may be useful for the design of devices that produce a coherent beam of bosonic atoms known as an atom laser.

Keywords: Bose–Einstein condensate; collapse–revival; macroscopic quantum self-trapping; population inversion.
DOI: 10.3788/COL202119.122701

1. Introduction

Nowadays a great deal of attention has been focused on the design of a device that produces a coherent beam of bosonic atoms known as an atom laser. Such devices are applicable in atom optics for various purposes, i.e., atom lithography, nano fabrication, and fundamental tests of quantum mechanics such as those involving atom interferometry[1]. The experimental realization of the Bose–Einstein condensate (BEC) results in the fast progress of atom optics due to the fact that a macroscopic number of atoms can be condensed in the ground state of an atomic trap that occupies a single quantum-mechanical state[2,3]. One of the most challenging problems in real many-particle systems is the coherent control of the interaction between the relevant particles.

The mean spacing between bosons is ten times greater than the range of inter-atomic forces due to the diluted nature of most BECs. In a BEC, the scattering length may possess either positive or negative values. The sign and magnitude of scattering length are of major importance, and they considerably affect the dynamics. A BEC with negative scattering length is composed of atoms with attractive interactions and implies the presence of a kind of wave solution called a bright soliton, which is a localized nonlinear wave against a zero background. On the other hand, a BEC with positive scattering length is repulsive and supports a different wave solution called a dark soliton. A dark soliton is also a localized nonlinear wave, but it is named dark because its magnitude implies a deficiency of the density with respect to a non-zero bulk value[4]. The scattering length depends on the atom species, but both the sign and magnitude may be manipulated via Feshbach resonance[5]. Experimentalists are able to manipulate atomic collisions and change the sign and strength of atomic interactions by tuning an external magnetic (or optical and electric) field in the vicinity of a Feshbach resonance[6,7]. Therefore, atomic BECs play the role of ideal experimental systems in different fields of quantum optics and particularly in continuous variable quantum information processing and teleportation[8,9]. The so-called macroscopic quantum self-trapping (MQST) is a phenomenon that manifests itself as a localization of most of particles in a particular space (region or quantum state) of a system[10–14]. The appearance of MQST becomes more pronounced with growing nonlinearity. Moreover, this effect plays an important role in the dynamics of condensates in periodic potentials and results in the formation of self-trapped or truncated gap states[15].

Based on the above-mentioned rich and interesting studies, we are motivated to investigate the effect of collisional interaction on the dynamics of ultra-cold Bosonic atoms and try to find under which conditions the pure quantum phenomena such as collapse–revival and MQST may take place in the dynamical

evolution of a system. The results show that our system shows a new kind of MQST, wherein the atoms mostly occupy a certain quantum state. Hereafter, we refer to this phenomenon as the MQST state (MQSTS). The occurrence of MQSTS, collapse–revival phenomena, and so their patterns strongly depend on the effect of nonlinear collisions and also the number of atoms in the system.

The remaining parts of this paper are organized as follows. In the next section, the model Hamiltonian and dynamics of the system are analyzed based on the Heisenberg approach. In section 3, the analytical expressions of population inversion are computed, considering two cases of number and coherent initial states, respectively. We also reanalyze the dynamics of the system via the time evolution operator in the absence and presence of inter-atomic collisions in this section. Our numerical results and discussions are presented in section 4. Finally, we summarize the results in the last section.

2. System and Its Model Hamiltonian

We consider a theoretical scheme to describe the interaction of a cloud of ultra-cold atoms with two classical radiation fields. The atoms possess three internal levels $|1\rangle$, $|2\rangle$, and $|3\rangle$ in the Λ configuration, where the two lower states $|1\rangle$ and $|2\rangle$ are coupled to the upper state $|3\rangle$ with two classical laser fields of frequencies ω_1 and ω_2, respectively. Usually, the atoms are confined in a three-dimensional isotropic harmonic trapping potential. Besides that, we suppose that the atoms interact with each other via elastic two-body collisions. Indeed, the collisions may be described via the δ-function potentials $V_{ij}(r-r') = U_{ij}\delta(r-r')$, where $U_{ij} = 4\pi\hbar^2 a_{ij}/m$ with m and a_{ij}, respectively, denoting the atomic mass and the s-wave scattering length between atoms in states i and j. A condensate consisting of sodium atoms with appropriate internal levels interacting with external laser fields is a good experimental candidate for our considered system[7,16,17]. As shown in Fig. 1, only the transitions $|1\rangle \leftrightarrow |3\rangle$ and $|2\rangle \leftrightarrow |3\rangle$ are allowed. On the other hand, the transition $|1\rangle \leftrightarrow |2\rangle$ is directly forbidden, but may take place through $|1\rangle \leftrightarrow |3\rangle \leftrightarrow |2\rangle$. In real physical systems, the confined cloud of BEC atoms is magnetically compressed and evaporatively cooled to a temperature where there is no noticeable non-condensed atomic fraction, i.e., less than 0.4 of the BEC transition temperature[18]. Thus, the results at zero temperature, like the one we obtain in this work, are valid for such experimental situations as well. Indeed, at very low temperatures, the s-wave scattering length can be used as a measure for the strength of the atom-atom interaction. Under typical experimental conditions, this interaction is weak and, hence, can be treated in terms of a mean field. However, when the scattering length is large or the density is high, the mean-field approximation breaks down. In this collisional (hydrodynamic) regime, the effects of the interactions such as quantum depletion or shifts in the frequencies of the elementary excitations become large. Therefore, it is of great interest to study condensates close to or in the collisional regime. The scattering length and thus the interactions among the atoms can be tuned by means of a Feshbach resonance; however, in the vicinity of Feshbach resonances, the increase of the cross section for elastic collisions is accompanied by a dramatic increase of particle losses[19]. Also, the quantum depletion is always present due to the interactions in the condensate. It should be noted that the ground state quantum depletion contributes to the density of atoms out of the condensate mode. Besides, the control of the external potential is another essential experimental technique in studying BEC. So far, various potentials have been implemented in laboratories, including magnetic traps, optical lattices, optical superlattices, double-well traps, and superpositions of lattices or superlattices with magnetic traps[20]. The shape and time variation of the external potential can be tuned accurately and flexibly, which enables different nonlinear waves and has been demonstrated in both experimental and theoretical studies[6].

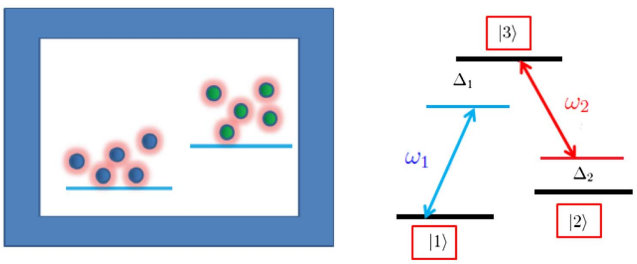

Fig. 1. Three-level atoms are in a Λ configuration, and the classical radiation fields have two different frequencies (right panel). Experimentally, such atomic systems consist of a binary mixture of BEC atoms, which are distributed in two hyperfine states and are transferred between them by the action of radiation fields[18] (left panel).

In practice, the collisional inter-atomic interactions, particle loss, and quantum depletion control (and may limit) the density of the BEC mode. In the present work that seeks the internal dynamics of BEC atoms, increasing the number of atoms may lead to the increase of the disorder (entropy). The increase of entropy and the conservation principles constitute the basic rules that govern the processes occurring in the universe. Notice that the essence of BEC is the perfect alignment of bosons[21]. Therefore, the entropy is the most important concept in BEC, which affects its dynamics dramatically. The dynamics of BEC atoms interacting with radiation fields at zero temperature, where there are no thermally excited atoms and the quantum depletion is negligible, can be described in the framework of the second quantization by the following model Hamiltonian:

$$\hat{H} = \sum_{i=1}^{3} \nu_i \hat{b}_i^\dagger \hat{b}_i - (g_1 \hat{b}_3^\dagger \hat{b}_1 e^{-i\omega_1 t} + g_2 \hat{b}_3^\dagger \hat{b}_2 e^{-i\omega_2 t} + \text{h.c.}) + \sum_{i=1}^{3} \lambda_i \hat{b}_i^{\dagger 2} \hat{b}_i^2 + \sum_{i\neq j}^{3} \lambda_{ij} \hat{b}_i^\dagger \hat{b}_i \hat{b}_j^\dagger \hat{b}_j, \quad (1)$$

where ν_i, $\hat{b}_i$, and $\hat{b}_i^\dagger$ are, respectively, the frequency, annihilation, and creation operators of BEC atoms in the states $|i\rangle$ $(i = 1, 2, 3)$.

The coupling constants g_1 and g_2 indicate the strengths of interaction between the BEC atoms and the classical radiation fields as described above. In the case of a traveling classical field, the explicit expression of coupling strengths can be written as $g_k = \varepsilon_k \mu_{ij}/\hbar\,(k = 1,2)$, where ε_k and μ_{ij} denote the amplitude of the classical field and the transition dipole-matrix element between the different states $|i\rangle$ and $|j\rangle$[22,23]. Also, λ_i and λ_{ij} $(i,j = 1,2,3)$ denote the strengths of nonlinear collisional interactions. The first line of Eq. (1) introduces the free Hamiltonians of the three-level atoms, while the second and last lines of Eq. (1) introduce the atom-field and collisional interactions in the system, respectively.

It should be noted that the above Hamiltonian provides a reasonably accurate picture for weak many-body interactions, i.e., for a small number of condensed atoms. Indeed, for large condensates, the mode functions of condensates are changed due to the collision interactions, especially when the number of atoms N satisfies $Na \gg r_0$, where a is a typical scattering length, and r_0 is a measure of the trap size. For instance, considering a large trap with the size $r_0 = 100$ m and the typical scattering length $a = 5$ nm, the Hamiltonian (which is derived based on the single-mode expansions of the atomic-field operators) is applicable for $N \leq 20{,}000$[17].

Anyway, based on Eq. (1), the time-independent Hamiltonian in the interaction picture is given as follows:

$$\hat{H}_I = \Delta_1 \hat{b}_3^\dagger \hat{b}_3 + (\Delta_1 - \Delta_2)\hat{b}_2^\dagger \hat{b}_2 - (g_1 \hat{b}_3^\dagger \hat{b}_1 + g_2 \hat{b}_3^\dagger \hat{b}_2 + \text{h.c.}) + \sum_{i=1}^{3} \lambda_i \hat{b}_i^{\dagger 2} \hat{b}_i^2 + \sum_{i \neq j}^{3} \lambda_{ij} \hat{b}_i^\dagger \hat{b}_i \hat{b}_j^\dagger \hat{b}_j, \tag{2}$$

where Δ_1 and Δ_2 are the frequency detunings of atoms with two respective classical laser beams. In the case of exact two-photon resonance, i.e., $\Delta = \Delta_1 = \Delta_2$, and also with large detuning condition $(\Delta \gg \nu_2 - \nu_1)$, one can adiabatically eliminate the atomic-field operators corresponding to the internal upper state $|3\rangle$[24]. Indeed, the experimental atomic BEC contains a binary mixture of ultra-cold atoms. The first realization of a binary mixture of condensates was produced by Myatt *et al.*[25] via overlapping the hyperfine levels $|F = 1, m_f = -1\rangle$ and $|F = 2, m_f = 2\rangle$ of ^{87}Rb[25]. Also, Matthews *et al.*[18] considered an ensemble of effective three-level atoms, where a virtual intermediate state connects the hyperfine states via a pulse of microwave radiation at a frequency slightly less than the ground state hyperfine splitting of ^{87}Rb ($\simeq 6.8$ GHz) along with a 2 MHz RF magnetic field. It should be noted that the virtual intermediate state can be adiabatically eliminated.

Therefore, the realistic BEC atom can be described by the following interaction Hamiltonian, which describes the transfer of atoms between two lower atomic states by the action of radiation fields, which is schematically depicted in the left panel of Fig. 1:

$$\hat{H}_I = \Omega_1 \hat{b}_1^\dagger \hat{b}_1 + \Omega_2 \hat{b}_2^\dagger \hat{b}_2 + (g_{\text{eff}} \hat{b}_2^\dagger \hat{b}_1 + g_{\text{eff}}^\star \hat{b}_1^\dagger \hat{b}_2) + \lambda_1 \hat{b}_1^{\dagger 2} \hat{b}_1^2 + \lambda_{12} \hat{b}_1^\dagger \hat{b}_1 \hat{b}_2^\dagger \hat{b}_2 + \lambda_2 \hat{b}_2^{\dagger 2} \hat{b}_2^2, \tag{3}$$

where we have defined $\Omega_1 = -|g_1|^2/\Delta$, $\Omega_2 = -|g_2|^2/\Delta$, and $g_{\text{eff}} = -g_1 g_2^\star/\Delta$.

In order to obtain the dynamical evolution of the system, we try to rewrite the Hamiltonian in Eq. (3) in terms of angular momentum operators, which are defined as

$$\hat{J}_+ = \hat{b}_2^\dagger \hat{b}_1, \quad \hat{J}_- = \hat{b}_1^\dagger \hat{b}_2, \quad \hat{J}_x = \frac{\hat{J}_+ + \hat{J}_-}{2}, \quad \hat{J}_y = \frac{\hat{J}_+ - \hat{J}_-}{2i}, \quad \hat{J}_z = \frac{1}{2}(\hat{b}_2^\dagger \hat{b}_2 - \hat{b}_1^\dagger \hat{b}_1), \tag{4}$$

and also $\hat{N} = \hat{b}_2^\dagger \hat{b}_2 + \hat{b}_1^\dagger \hat{b}_1$, which denotes the total number of operators. Using the above operators, we arrive at the effective Hamiltonian as

$$\hat{H}_{\text{eff}} = (g_{\text{eff}} \hat{J}_+ + g_{\text{eff}}^\star \hat{J}_-) + [\Omega_2 - \Omega_1 + (N-1)(\lambda_2 - \lambda_1)]\hat{J}_z + (\lambda_1 + \lambda_2 - \lambda_{12})\hat{J}_z^2, \tag{5}$$

where the constant energy terms containing $\hat{N}$ and $\hat{N}^2$ have been removed[22]. Assuming real coupling constants $G = 2|g_{\text{eff}}| = 2|g_{\text{eff}}^\star|$, the simplified form of the effective Hamiltonian can be expressed as follows:

$$\hat{H}_{\text{eff}} = A\hat{J}_z + 2B\hat{J}_z^2 + G\hat{J}_x, \tag{6}$$

where we have set $A = [\Omega_2 - \Omega_1 + (N-1)(\lambda_2 - \lambda_1)]$ and $B = \frac{1}{2}(\lambda_1 + \lambda_2 - \lambda_{12})$. Now, we intend to investigate the dynamics of the system by considering two different initial conditions. For simplicity, we assume $A = 0$, which can be realized by adjusting the atomic frequency difference $\Omega_2 - \Omega_1$, the total number of atoms N in the system, and the collisional interaction constants, i.e., λ_2 and λ_1, all of which are experimentally accessible. Also, the so-called RWA can be adapted whenever the Rabi frequency G is larger than the frequency of the magnetic trap[26] to provide a BEC system. Such physical conditions have previously been used to study the dynamical evolution of two-mode BEC systems[27,28].

3. Dynamics of the System: Population Inversion

In this section, we study population inversion as a key quantity to investigate the dynamics of our BEC system. This quantity is usually used to extract the information of energy transfer between atoms and photons, i.e., the internal dynamics of the system. In this regard, we define the operators $\hat{J}_1 = \hat{J}_z + i\hat{J}_y$ and $\hat{J}_2 = \hat{J}_z - i\hat{J}_y$. Using the Heisenberg equation of motion $\{\dot{\hat{J}}_l(t) = -i[\hat{J}_l(t), \hat{H}_{\text{RWA}}]$, where $\hat{H}_{\text{RWA}} = -B\hat{J}_x^2 + G\hat{J}_x\}$, the time evolution of the mentioned operators are easily obtained as

$$\hat{J}_1(t) = e^{i(2B\hat{J}_x + B - G)t}\hat{J}_1(0), \quad \hat{J}_2(t) = e^{i(-2B\hat{J}_x + B + G)t}\hat{J}_2(0). \tag{7}$$

These relations can be used to study the dynamics of the system. The population inversion of the system can be defined as

$$W(t) = \langle\Psi(0)|\hat{N}_2(t) - \hat{N}_1(t)|\Psi(0)\rangle$$
$$= \langle\Psi(0)|e^{-2iB\hat{J}_x t}\hat{J}_2(0)|\Psi(0)\rangle e^{i(G+B)t} + \text{c.c}, \quad (8)$$

where we have used the relation $2\hat{J}_z(t) = \hat{b}_2^\dagger(t)\hat{b}_2(t) - \hat{b}_1^\dagger(t)\hat{b}_1(t)$. In the continuation, we consider two different kinds of initial states for BEC atoms. As the first case, we consider that all atoms populate the state $|2\rangle$, which can be defined as a Fock number state $|N\rangle$, while state $|1\rangle$ is empty. Accordingly, the initial state of the system can be written as $|0,N\rangle$, which is possible to be expressed in terms of the angular momentum state $|j,j\rangle$ with $j = N/2$.

3.1. Number state case

In order to obtain analytical expressions of population inversion, we insert the initial state $|j,j\rangle$ in Eq. (8) and proceed as follows:

$$W(t) = \langle j,j|e^{-i\frac{\pi}{2}\hat{J}_y}e^{-2iB\hat{J}_z t}\hat{J}_+ e^{i\frac{\pi}{2}\hat{J}_y}|j,j\rangle \times e^{i(G+B)t} + \text{c.c}$$
$$= \sum_{m=-j}^{j}\sum_{m'=-j}^{j}\langle j,j|e^{-i\frac{\pi}{2}\hat{J}_y}|j,m\rangle \times \langle j,m|e^{-2iB\hat{J}_z t}\hat{J}_+|j,m'\rangle$$
$$\times \langle j,m'|e^{i\frac{\pi}{2}\hat{J}_y}|j,j\rangle e^{i(G+B)t} + \text{c.c}, \quad (9)$$

where we have set

$$e^{-iA\hat{J}_x t}\hat{J}_2(0) = e^{-i\frac{\pi}{2}\hat{J}_y}e^{-iA\hat{J}_z t}\hat{J}_+(0)e^{i\frac{\pi}{2}\hat{J}_y}.$$

Equation (9) can be simplified as

$$W(t) = \frac{1}{2^N}e^{i(G+B)t}\sum_{m=-j}^{j}(j+m)\binom{2j}{j+m}e^{-2iBmt} + \text{c.c}. \quad (10)$$

For $N = 2$ and using Eq. (10), one can easily compute the population inversion as below,

$$W(t) = \frac{1}{2^2}e^{i(G+B)t}\left(0\binom{2}{0} + 1\binom{2}{1} + 2\binom{2}{2}e^{-2iBt}\right) + \text{c.c}$$
$$= 2\cos Bt\cos Gt. \quad (11)$$

Therefore, the analytical expression of population inversion for a system containing N atoms with initial number state can be obtained as

$$W_{\text{num}}(t) = N(\cos Bt)^{N-1}\cos Gt, \quad (12)$$

where G and B have been defined earlier. From the analytical expression of population inversion in Eq. (12), we are able to find a few prominent features. It should be noticed that population inversion possesses two distinct factors. The first feature may be attributed to its slow-varying factor. We expect that the envelope function $(\cos Bt)^{N-1}$ results in the collapse–revival phenomenon, while the oscillatory factor of Eq. (12) including $\cos Gt$ implies the usual Rabi oscillation of frequency G. Also, the MQSTS is another considerable feature that strongly depends the total number of atoms in the system. For the sake of simplicity of analysis, we consider a particular case wherein $G = B$. If the number of atoms is even, the revival period is π/B, and therefore population inversion always possesses positive values, i.e., $\langle W(t)\rangle \neq 0$, which demonstrates the occurrence of MQSTS. On the other hand, whenever N is odd, the population undergoes anti-revival. In this case, the revival period becomes $2\pi/B$. In general, the revival time can be tuned by adjusting the ratio of strengths of interactions, i.e., G/B as well as the total number of atoms in the system, N.

3.2. Coherent state case

As the second case, we replace the atomic number state with its coherent counterpart. Now, we consider a two-mode standard coherent state as

$$|\Psi(0)\rangle = |\alpha,\beta\rangle, \quad |Z\rangle = e^{\frac{-|Z|^2}{2}}\sum_{j=0}^{\infty}\frac{Z^j}{\sqrt{j!}}|j\rangle, \quad Z = \alpha,\beta, \quad (13)$$

and follow the computation as

$$W(t) = \langle\Psi(0)|e^{-2iB\hat{J}_x t}\hat{J}_2(0)|\Psi(0)\rangle e^{i(G+B)t} + \text{c.c}. \quad (14)$$

For the sake of simplicity, we exchange $\hat{J}_x \leftrightarrow \hat{J}_z$ and also $\hat{J}_y \to -\hat{J}_y$, and rewrite Eq. (14) as below,

$$W(t) = \langle\Psi(0)|e^{-2iB\hat{J}_z t}\hat{J}_+|\Psi(0)\rangle e^{i(G+B)t} + \text{c.c}. \quad (15)$$

Inserting Eq. (13) into Eq. (15) and after some simplifications, we arrive at

$$W(t) = e^{i(G+B)t}\alpha\beta^* e^{-|\alpha|^2-|\beta|^2}\times\sum_{n=0}^{\infty}\sum_{m=0}^{\infty}e^{iBt(n-m)}\frac{|\alpha|^{2n}|\beta|^{2n}}{n!m!} + \text{c.c}. \quad (16)$$

For the case of $\beta = \alpha e^{i\phi}$, where ϕ is the relative phase of the considered two-mode coherent state, the above expression can be rewritten as

$$W(t) = 2|\alpha|^2 e^{-4|\alpha|^2\sin^2\frac{Bt}{2}}\cos[(G+B)t - \phi]. \quad (17)$$

Now, in the case of $G \gg B$ and for $\phi = 0$, we obtain the final expression of population inversion with the initial coherent state,

$$W_{\text{coh}}(t) = \bar{N}e^{-2\bar{N}\sin^2\frac{Bt}{2}}\cos Gt, \quad (18)$$

where we have set $\bar{N} = \frac{|\alpha|^2}{2}$. It is worthwhile to note that the dynamics of the system are drastically influenced by the nonlinear collisional interactions. Equations (12) and (18) clearly demonstrate that in the absence of inter-atomic interaction ($B = 0$), population inversion undergoes a harmonic oscillatory evolution, and the atoms are regularly transferred between two states

by the action of radiation fields. As is clear, in this case, we do not expect to observe quantum phenomena, i.e., the collapse–revival pattern and MQSTS. Indeed, the essence of these pure quantum phenomena is the nonlinear collisional interactions.

3.3. Unitary time evolution operator approach beyond RWA

In this subsection, we want to investigate the dynamics of the system using the time evolution operator approach without considering RWA. Since the general behavior of the system is similar for both number and coherent state cases, here we only obtain the dynamics of the system with the initial number state.

• The exact state vector of the system

We rewrite the Hamiltonian in Eq. (6) as below,

$$\hat{H}_{\rm eff} = A\hat{J}_z + 2B\hat{J}_z^2 + \frac{G}{2}(\hat{J}_+ + \hat{J}_-). \tag{19}$$

In the absence of nonlinear collisions ($B=0$), the above Hamiltonian in the interaction picture can be expressed as

$$\hat{H}_{\rm int} = e^{i\hat{H}_0 t}\hat{H}_1 e^{-i\hat{H}_0 t} = \frac{G}{2}(\hat{J}_+ e^{iAt} + \hat{J}_- e^{-iAt}), \tag{20}$$

where we have used $\hat{H}_0 = A\hat{J}_z$ and $\hat{H}_1 = \frac{G}{2}(\hat{J}_+ + \hat{J}_-)$. In the case of $A=0$, the time evolution operator corresponding to the Hamiltonian of Eq. (20) can be computed as $\hat{U}(t) = e^{\chi\hat{J}_+ - \chi^*\hat{J}_-}$ with $\chi = iqt$ and $q = G/2$. Once again, the initial state of the system is chosen as $|j,j\rangle$, similar to the number state case. Therefore, the time-dependent state of the system during the interaction can be obtained as

$$|\Phi(t)\rangle = \sum_{m=-j}^{j}\sqrt{\frac{(2j)!}{(j-m)!(j+m)!}} \times (\cos qt)^{j+m}(\sin qt)^{j-m}e^{i(j-m)\frac{\pi}{2}}|j,m\rangle. \tag{21}$$

This is a generalized coherent state associated with the unitary representations of the Su(2) algebra or atomic coherent state, which is parameterized by the two polar angles in $\zeta = \theta/2e^{-i\phi}$ with $\theta/2 = qt$ and with fixed ϕ at $\pi/2$. The general form of the atomic coherent state can be defined as $|\theta,\phi\rangle = D(\zeta)|j,-j\rangle$ with $D(\zeta) = \exp(\zeta\hat{J}_+ - \zeta^*\hat{J}_-)$[29]. Therefore, we have briefly set $|\Phi(t)\rangle = |\theta = 2qt, \phi = \pi/2\rangle$.

• The perturbed state vector of the system

In the presence of inter-atomic nonlinear collisions, the interaction Hamiltonian can be obtained as

$$\hat{H}_{\rm int} = q\{\hat{J}_+ e^{i[A+B(2\hat{J}_z+1)]t} + \hat{J}_- e^{-i[A+B(2\hat{J}_z+1)]t}\}. \tag{22}$$

In this case, the exact dynamical evolution for the system cannot be found due to the presence of the operator $\hat{J}_z$ in nonlinear terms in Eq. (22). Therefore, we proceed to apply the perturbation theory and use the time evolution operator,

$$\hat{U}(t) = 1 - i\int_0^t {\rm d}t'\hat{H}_{\rm int}(t) - \int_0^t {\rm d}t'\hat{H}_{\rm int}(t)\int_0^{t'} {\rm d}t''\hat{H}_{\rm int}(t'') + \cdots. \tag{23}$$

The time evolution operator up to the second-order perturbation can be computed as below,

$$\begin{aligned}\hat{U}(t) = 1 &- \frac{q}{\hat{\Gamma}}[(e^{i\hat{\Gamma}t} - 1)\hat{J}_+ - (e^{-i\hat{\Gamma}t} - 1)\hat{J}_-] \\ &+ \frac{q^2}{2\hat{\Gamma}^2(\hat{\Gamma} - B)}\{\hat{\Gamma}[1 + e^{2i(\hat{\Gamma}-B)t} - 2e^{i\hat{\Gamma}t}] + 2B(e^{i\hat{\Gamma}t} - 1)\}\hat{J}_+^2 \\ &+ \frac{q^2}{2\hat{\Gamma}^2 B}[\hat{\Gamma}(1 - e^{2iBt}) + 2B(e^{i\hat{\Gamma}t} - 1)]\hat{J}_+\hat{J}_- \\ &+ \frac{q^2}{2\hat{\Gamma}^2 B}[\hat{\Gamma}(e^{2iBt} - 1) + 2B(e^{-i\hat{\Gamma}t} - 1)]\hat{J}_-\hat{J}_+ \\ &- \frac{q^2}{2\hat{\Gamma}^2(\hat{\Gamma} + B)}\{\hat{\Gamma}[2e^{-i\hat{\Gamma}t} - e^{2i(\hat{\Gamma}+B)t} - 1] \\ &+ 2B(e^{-i\hat{\Gamma}t} - 1)\}\hat{J}_-^2,\end{aligned} \tag{24}$$

where we have set $\hat{\Gamma} = A + B(2\hat{J}_z + 1)$. Therefore, the state vector of the system after the action of the time evolution operator, i.e., $|\Psi(t)\rangle = \hat{U}(t)|j,j\rangle$, can be explicitly obtained as

$$|\Psi(t)\rangle = \frac{1}{\mathcal{N}(t)}[A(t)|j,j\rangle + B(t)|j,j-1\rangle + C(t)|j,j-2\rangle], \tag{25}$$

where

$$\begin{aligned}A(t) &= 1 + \frac{jq^2}{\alpha_1^2 B}[\alpha_1(1 - e^{2iBt}) + 2B(e^{i\alpha_1 t} - 1)], \\ B(t) &= \frac{\sqrt{2j}q}{\alpha_2}(e^{-i\alpha_2 t} - 1), \\ C(t) &= -\frac{\sqrt{j(2j-1)}q^2}{\alpha_3^2(\alpha_3 + B)} \\ &\quad\times\{\alpha_3[2e^{-i\alpha_3 t} - e^{-2i(\alpha_3+B)t} - 1] + 2B(e^{-i\alpha_3 t} - 1)\}, \\ \mathcal{N}(t) &= [|A(t)|^2 + |B(t)|^2 + |C(t)|^2]^{1/2},\end{aligned} \tag{26}$$

with definitions $\alpha_1 = f(j)$, $\alpha_2 = f(j-1)$, $\alpha_3 = f(j-2)$, and $f(j) = A + B(2j+1)$. Here, it is worth noting that the first-order perturbed terms of the time evolution operator of Eq. (24) are proportional to $\frac{q}{\hat{\Gamma}} \simeq \frac{G/2}{A+NB}$. For the sake of simplicity, for $A=0$ (as discussed in the second section) and considering $G \ll NB$, especially in the strong excitation condition, one arrives at $\frac{q}{\hat{\Gamma}} \simeq \frac{G}{2NB} \ll 1$. Also, the second-order terms contain $\frac{q^2}{\hat{\Gamma}^2} \simeq \frac{G^2}{4N^2B^2} \ll \frac{G}{2NB}$. Therefore, the leading terms in the expansion of the time evolution operator include up to second-order perturbed terms.

3.4. Exact and perturbed analytical expressions of population inversion beyond RWA

As mentioned above, the population inversion is defined as the expectation value of the z component of the angular momentum operator. Using the state of Eq. (21), the exact analytical expression of population inversion in the absence of nonlinear interaction can be obtained as

$$W_{\Phi}(t) = 2\langle\Phi(t)|\hat{J}_z|\Phi(t)\rangle = \sum_{j=-m}^{m} \frac{2\,m(2j)!}{(j+m)!(j-m)!}(\cos\, qt)^{j+m}(\sin\, qt)^{j-m}, \quad (27)$$

while, in the presence of nonlinear collisions via considering the state in Eq. (25), one can derive the population inversion as

$$W_{\Psi}(t) = 2\langle\Psi(t)|\hat{J}_z|\Psi(t)\rangle = \frac{2}{\mathcal{N}^2(t)}[j|A(t)|^2 + (j-1)|B(t)|^2 + (j-2)|C(t)|^2]. \quad (28)$$

4. Numerical Results and Discussion

Here, we investigate the dynamics of the system qualitatively. Thus, we choose scaled parameters and a small number of atoms. Nevertheless, by rescaling the involved parameters in the model, one can consider more real physical conditions, i.e., a larger number of atoms (such a small number of atoms in the BEC has also been considered in typical works in the literature[30,31]).

Figure 2 shows the time evolution of atomic inversion against the scaled time $\tau = Bt$ for two initial number and coherent states. One can clearly observe that the atomic inversion undergoes the collapse–revival phenomenon. The period of revivals in the coherent state case is twice the cases of the number state, which can be found from the comparison of slowly varying parts of atomic inversion in the number and coherent state cases resulted from $(\cos\, Bt)^{N-1}$ and $e^{-2\bar{N}\sin^2\frac{Bt}{2}}$, respectively. Indeed, the periods of revivals in the number state and coherent state cases are $T_N = \pi/B$ and $T_C = 2\pi/B$, respectively. Two distinct revival periods corresponding to the number and coherent state cases, i.e., T_N and T_C originate from the fact that the atom number difference operator $\hat{b}_2^{\dagger}\hat{b}_2 - \hat{b}_1^{\dagger}\hat{b}_1$ is quantized in units of two for condensates in number states and in units of one for coherent states[32]. Therefore, we conclude that the atomic inversion for both number and coherent cases possesses similar behavior, and also the collapse–revival phenomenon may occur due to the presence of nonlinear collisions in the system. This phenomenon declares itself in some related interacting systems, i.e., the two-mode BEC system, wherein the collisional interactions drastically influence the dynamics of the system[30]. In addition, the usual atom-field interaction described by the Jaynes–Cummings model may result in the collapse–revival phenomenon, especially when the atoms begin the interaction with the coherent field. In this case, the granular structure of photon distribution is the origin of this phenomenon[22].

Now, we are interested to find out how the strength of the atom-field interaction affects the dynamics of the system. So, we study population inversion in the system under the influence of various interaction regimes. As is demonstrated in Fig. 3, the various values of coupling strength of interaction (G) result in different dynamical behaviors, i.e., transitions from oscillation to MQSTS and also the collapse–revival phenomenon. As shown in Fig. 3(a), for relatively weak coupling constant (i.e., $G = 2\,B$), population inversion shows a regular oscillatory pattern, which possesses both positive and negative values, meaning that the atoms move from a level to another one ($|1\rangle \leftrightarrow |2\rangle$). Choosing a stronger coupling constant such as $G = 3B$, one can observe that the inversion oscillates just with positive amplitude, which implies that the atoms are localized in one atomic

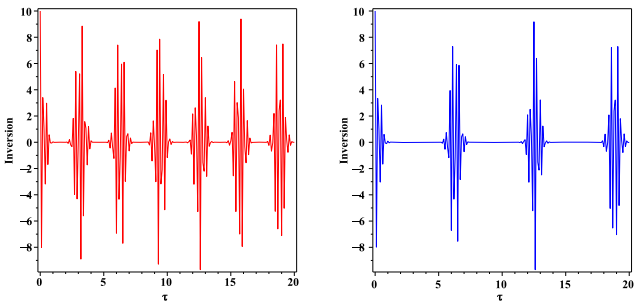

(a) Initial number state (b) Initial coherent state

Fig. 2. Effect of initial state on the time evolution of population inversion for $N = \bar{N} = 10$ and $G = 100B$ with scaled time $\tau = Bt$.

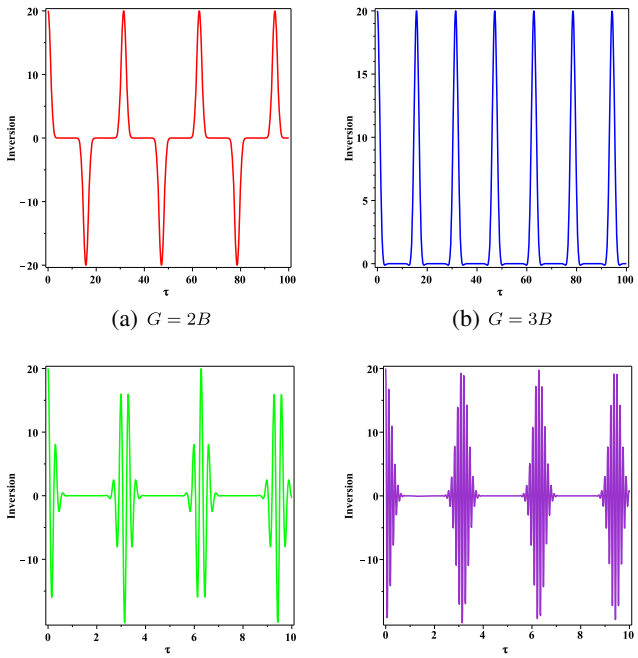

(a) $G = 2B$ (b) $G = 3B$

(c) $G = 20B$ (d) $G = 50B$

Fig. 3. Effect of G on the time evolution of population inversion in the case of number state versus the scaled time $\tau = Bt$ with $N = 20$.

level. In the following, we discuss more of this physical situation. For $G = 20B$, the population inversion again oscillates between positive and negative values. Therefore, we can conclude that the atomic localization has been removed in Fig. 3(c). Also, the collapse–revival pattern can be seen in the pattern of population dynamics. By further increasing the coupling strength to the value $G = 50B$, the collapse–revival phenomenon becomes more pronounced. Generally, we can state that the atom-field coupling strength G considerably affects the pattern of population inversion and may lead to various quantum phenomena in the dynamics of the system. In addition, the frozen behavior of population inversion can be understood when the Rabi frequency (G) is sufficiently larger than nonlinear collisional interaction strength B. In this case, the external fields force the atoms to be polarized in a defined direction, and one can expect that the general pattern of the population remains unchanged by further increasing the Rabi frequency. In this condition, the system is more stable, and the RWA is more reliable.

From Eqs. (12) and (18), it can be found that atomic inversion is very sensitive to the number of atoms in the system. Accordingly, we study the effect of the number of atoms on the dynamical evolution system in Fig. 4 for the cases of number and perturbed states. Once the number of atoms is odd, for instance in Fig. 4(a), atomic inversion has both positive and negative values. On the other hand, whenever the number of atoms in the system is even shown in Fig. 4(b), the population inversion only possesses the positive values, which indicates the MQSTS phenomenon as mentioned above. In addition, the effect of second-order perturbation on the dynamics of the system has been presented in each plot. In fact, using the second-order perturbed state and by increasing the number of atoms in the system, one can observe that the amplitude of atomic inversion considerably decreases, and the MQSTS phenomenon becomes more pronounced. Indeed, one can conclude that by increasing the number of atoms, the system shows more excitations due to collisional inter-atomic interactions. Also, the pattern of the typical collapse–revival phenomenon can be seen for a larger

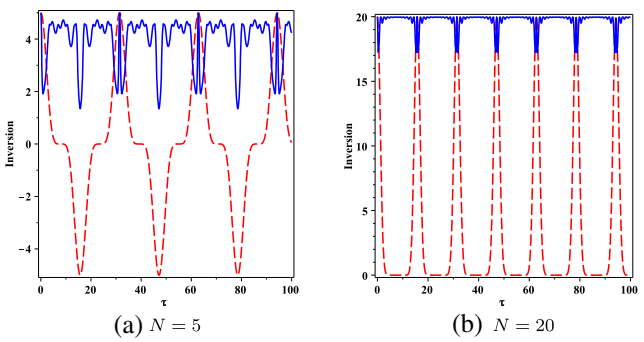

(a) $N = 5$ (b) $N = 20$

Fig. 4. Evolution of population inversion for the number state (dash lines) and perturbed state (solid lines) against the scaled time $\tau = At$, when $B = 0.2A$ for different numbers of atoms in the system. The parity of number of atoms considerably affects the behavior of population inversion. The even parity leads to MQSTS phenomenon.

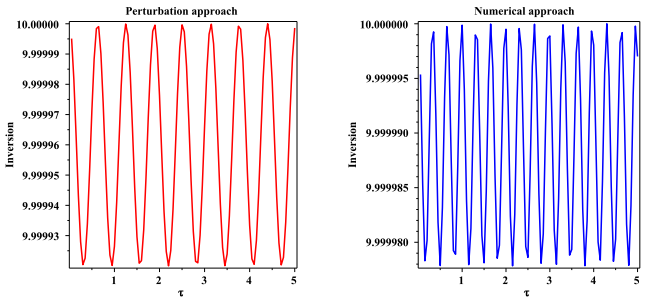

(a) Perturbation (b) Numerical

Fig. 5. Comparison between the results of the perturbation method and numerical solution of the Schrödinger equation for $N = 10$, $B = A = 100q$, and $\tau = At$.

number of atoms in the system, particularly in the second plot of Fig. 4.

In this section, it would be useful to check the accuracy of the results of perturbation. In this regard, we compare the population inversion obtained by the perturbation method with the numerical result of the solution of the Schrödinger equation corresponding to the Hamiltonian in Eq. (6). In order to solve the Schrödinger equation, we consider a state vector for the system as $|\psi_{\mathrm{Sch}}(t)\rangle = K_1(t)|j,j\rangle + K_2(t)|j,j-1\rangle + K_3(t)|j,j-2\rangle$ in analogy to Eq. (25). After obtaining the time-dependent coefficients $K_i(t)$ for $i = 1,2,3$, we numerically compute the population inversion using $W_{\mathrm{Sch}}(t) = 2\langle\psi_{\mathrm{Sch}}(t)|\hat{J}_z|\psi_{\mathrm{Sch}}(t)\rangle$. Figure 5 shows the results of population inversion obtained via the perturbation approach and numerical method, respectively. As can be observed from Figs. 5(a) and 5(b), the perturbation results up to the second-order are in agreement with the numerical solution. Both methods present the same pattern with good accuracy, however, a small difference between their frequencies exists, which may be improved by considering higher-order perturbed terms and choosing the relevant state vector for numerical computations.

5. Summary and Conclusion

We investigated the dynamics of a BEC system consists of N three-level atoms with a Λ configuration interacting with two classical radiation fields. Indeed, we studied the dynamics of population inversion by considering different physical situations. Our theoretical and numerical results demonstrated that the system undergoes the collapse–revival and MQSTS phenomena. The period of revival and also the pronouncement of MQSTS depend on the number of atoms in the system as well as the parameters describing the interactions between the components of the system. Furthermore, it was shown that the dynamical evolution of population inversion experiences transitions from regular oscillation to collapse–revival and MQSTS phenomena. Based on the presented results, atomic collisions play a key role in the dynamics of BEC atoms; therefore, such nonlinear interactions are of fundamental interest for the

design and fabrication of devices that produce and deal with coherent atomic beams such as atom lasers and atomic interferometers.

References

1. M. Holland, K. Burnett, C. Gardiner, J. I. Cirac, and P. Zoller, "Theory of an atom laser," Phys. Rev. A **54**, R1757 (1996).
2. M. H. Anderson, J. R. Ensher, M. R. Matthews, C. E. Wieman, and E. A. Cornell, "Observation of Bose–Einstein condensation in a dilute atomic vapor," Science **269**, 198 (1995).
3. C. C. Bradley, C. A. Sackett, J. J. Tollett, and R. G. Hulet, "Evidence of Bose–Einstein condensation in an atomic gas with attractive interactions," Phys. Rev. Lett. **75**, 1687 (1995).
4. L. Pitaevskii and S. Stringari, *Bose–Einstein Condensation* (Clarendon, 2003).
5. T. Dauxois and M. Peyrard, *Physics of Solitons* (Cambridge University, 2005).
6. R. Carretero-Gonzalez, D. J. Frantzeskakis, and P. G. Kevrekidis, "Nonlinear waves in Bose–Einstein condensates: physical relevance and mathematical techniques," Nonlinearity **21**, R139 (2008).
7. L. M. Kuang, A. H. Zeng, and Z. H. Kuang, "Generation of entangled squeezed states in atomic Bose–Einstein condensates," Phys. Lett. A **319**, 24 (2003).
8. H. Jeong and M. S. Kim, "Efficient quantum computation using coherent states," Phys. Rev. A **65**, 042305 (2002).
9. S. J. van Enk and O. Hirota, "Entangled coherent states: teleportation and decoherence," Phys. Rev. A **64**, 022313 (2001).
10. M. Abbarchi, A. Amo, V. G. Sala, D. D. Solnyshkov, H. Flayac, L. Ferrier, I. Sagnes, E. Galopin, A. Lemaître, G. Malpuech, and J. Bloch, "Macroscopic quantum self-trapping and Josephson oscillations of exciton polaritons," Nat. Phys. **9**, 275 (2013).
11. S. Raghavan, A. Smerzi, S. Fantoni, and S. R. Shenoy, "Coherent oscillations between two weakly coupled Bose–Einstein condensates: Josephson effects, π oscillations, and macroscopic quantum self-trapping," Phys. Rev. A **59**, 620 (1999).
12. E. Ghasemian and M. K. Tavassoly, "Population imbalance, macroscopic tunneling and intermodal entanglement of two-mode Bose–Einstein condensate under the influence of dissipation process," Int. J. Mod. Phys. B **33**, 1950181 (2019).
13. E. Ghasemian and M. K. Tavassoly, "Dissipative evolution of two-mode Bose–Einstein condensate in the presence of nonlinear interactions: Heisenberg operator approach," Phys. A: Stat. Mech. Appl. **514**, 715 (2019).
14. E. Ghasemian and M. K. Tavassoly, "Spontaneous emission originating from atomic BEC interacting with a single-mode quantized field," Commun. Theor. Phys. **69**, 711 (2018).
15. T. J. Alexander, E. A. Ostrovskaya, and Y. S. Kivshar, "Self-trapped nonlinear matter waves in periodic potentials," Phys. Rev. Lett. **96**, 040401 (2006).
16. S. Inouye, R. F. Löw, S. Gupta, T. Pfau, A. Görlitz, T. L. Gustavson, D. E. Pritchard, and W. Ketterle, "Amplification of light and atoms in a Bose–Einstein condensate," Phys. Rev. Lett. **85**, 4225 (2000).
17. L. V. Hau, S. E. Harris, Z. Dutton, and C. H. Behroozi, "Light speed reduction to 17 metres per second in an ultracold atomic gas," Nature **397**, 594 (1999).
18. M. R. Matthews, D. S. Hall, D. S. Jin, J. R. Ensher, C. E. Wieman, and E. A. Cornell, "Dynamical response of a Bose–Einstein condensate to a discontinuous change in internal state," Phys. Rev. Lett. **81**, 243 (1998).
19. J. Schuster, A. Marte, S. Amtage, B. Sang, G. Rempe, and H. C. W. Beijerinck, "Critical collisional opacity in a Bose–Einstein condensate," in *Quantum Electronics and Laser Science Conference, Postconference Technical Digest* (IEEE, 2001), p. 236.
20. M. A. Porter and P. G. Kevrekidis, "Bose–Einstein condensates in superlattices," SIAM J. Appl. Dynam. Syst. **4**, 783 (2005).
21. P. L. You, "Bose–Einstein condensation in a vapor of sodium atoms in an electric field," Phys. B **491**, 84 (2016).
22. M. O. Scully and M. S. Zubairy, *Quantum Optics* (Cambridge University, 1997).
23. W. P. Schleich, *Quantum Optics in Phase Space* (Wiley-VCH, 2001).
24. L.-M. Kuang and L. Zhou, "Generation of atom-photon entangled states in atomic Bose–Einstein condensate via electromagnetically induced transparency," Phys. Rev. A **68**, 043606 (2003).
25. C. J. Myatt, E. A. Burt, R. W. Ghrist, E. A. Cornell, and C. E. Wieman, "Production of two overlapping Bose–Einstein condensates by sympathetic cooling," Phys. Rev. Lett. **78**, 586 (1997).
26. J. Williams, R. Walser, J. Cooper, E. A. Cornell, and M. Holland, "Excitation of a dipole topological state in a strongly coupled two-component Bose–Einstein condensate," Phys. Rev. A **61**, 033612 (2000).
27. L. M. Kuang, Z. Y. Tong, Z. W. Ouyang, and H. S. Zeng, "Decoherence in two Bose–Einstein condensates," Phys. Rev. A **61**, 013608 (1999).
28. G.-R. Jin, Z.-X. Liang, and W.-M. Liu, "Collapses and revivals of exciton emission in a semiconductor microcavity," J. Opt. B: Quantum Semiclassical Opt. **6**, 296 (2004).
29. G. S. Agarwal, *Quantum Optics* (Cambridge University, 2013).
30. L.-M. Kuang and Z.-W. Ouyang, "Macroscopic quantum self-trapping and atomic tunneling in two-species Bose–Einstein condensates," Phys. Rev. A **61**, 023604 (2000).
31. Z. Haghshenasfard, M. H. Naderi, and M. Soltanolkotabi, "The influence of atomic collisions on collective spontaneous emission from an *f*-deformed Bose–Einstein condensate," J. Phys. B: Atom. Mol. Opt. Phys. **42**, 065505 (2009).
32. T. Wong, M. J. Collet, S. M. Tan, D. F. Walls, and E. M. Wright, "Tests of Bose-broken symmetry in atomic Bose–Einstein condensates," arXiv: cond-mat/9611101 (1996).